Drop Growth Due to High Supersaturation Caused by Isobaric Mixing

ALEXEI V. KOROLEV AND GEORGE A. ISAAC

Meteorological Service of Canada, Toronto, Ontario, Canada

(Manuscript received 16 December 1998, in final form 25 June 1999)

ABSTRACT

A new conceptual model is proposed for enhanced cloud droplet growth during condensation. Rapid droplet growth may occur in zones of high supersaturation resulting from isobaric mixing of saturated volumes with different temperatures. Cloud volumes having a temperature different from the general cloud environment may form due to turbulent vertical motions in a temperature lapse rate that is not pseudoadiabatic. This mechanism is most effective in the vicinity of cloud-top inversions. It is also shown that the isobaric mixing of saturated and dry volumes with different temperatures may also lead to high supersaturations. The high supersaturations are associated with zones of molecular mixing, and they have a characteristic size of the order of millimeters with a characteristic lifetime near tenths of a second. Some small proportion of cloud droplets, over many supersaturation events, may grow large enough to grow effectively through collision–coalescence. This hypothesis of isobaric mixing may help explain freezing and warm drizzle formation.

1. Introduction

Supersaturation in clouds is one of the principal parameters controlling droplet growth during condensation. The shape of the droplet size distribution formed during condensation strongly affects the further evolution of the ensemble of droplets through collision–coalescence and the formation of precipitation size drops. Supersaturation in clouds is considered to be a result of the following processes: 1) vertical motions, 2) entrainment and mixing of dry out-of-cloud air, 3) radiative cooling or heating, and 4) condensation and evaporation of droplets. In the present study, we consider isobaric mixing as another potential source of supersaturation that may play an important role in cloud microstructure formation. Isobaric mixing in certain conditions may result in zones with a high supersaturation that may lead to rapid growth of large droplets and accelerate precipitation formation.

2. Isobaric mixing of two saturated volumes

It is well known that isobaric mixing of two saturated volumes having different temperatures results in a higher supersaturation than in either of these volumes (e.g., Rogers 1976; Bohren and Albreht 1998). Let us consider isobaric mixing of two volumes at pressure P, having initial temperatures T_1 and T_2, and water vapor pressure E_1 and E_2, respectively. The supersaturation resulting from the mixing will be

$$S_m = \frac{E_m}{E_S(T_m)} - 1. \tag{1}$$

Here, $E_S(T_m)$ is the saturated water vapor pressure at temperature T_m; T_m and E_m are the temperature and water vapor pressure, respectively, resulting from the mixing of two volumes (appendix A):

$$T_m = \frac{kT_1 + a(1-k)T_2}{k + a(1-k)}; \tag{2}$$

$$E_m = P\left(k + \frac{E_2(P-E_1)}{P(E_1-E_2)}\right)\Bigg/\left(k + \frac{(P-E_1)}{(E_1-E_2)}\right); \tag{3}$$

$$a = \left(1 + \frac{c_{pv}R_aE_2}{c_{pa}R_v(P-E_2)}\right)\Bigg/\left(1 + \frac{c_{pv}R_aE_1}{c_{pa}R_v(P-E_1)}\right). \tag{4}$$

Here, k is the portion (ratio of mixing) of the first volume mixed with the $(1-k)$ portion of the second volume, both volumes having a unit mass of dry air, R_v, R_a, which are specific gas constants of water vapor and dry air, respectively. Constants c_{pv}, c_{pa} are the specific heat capacitance of water vapor and dry air at constant pressure, respectively.

Figure 1 shows the resulting supersaturation and temperature versus the ratio of mixing (k) for different temperatures in the mixing parcels. A maximum in supersaturation is reached when k is close to 0.5, and it decreases with a decrease in the temperature difference. Figure 2 shows the maximum supersaturation that can

Corresponding author address: Dr. Alexei V. Korolev, Cloud Physics Research Division, Meteorological Service of Canada, 4905 Dufferin Street, Toronto, ON M3H 5T4, Canada.
E-mail: alexei.korolev@ec.gc.ca

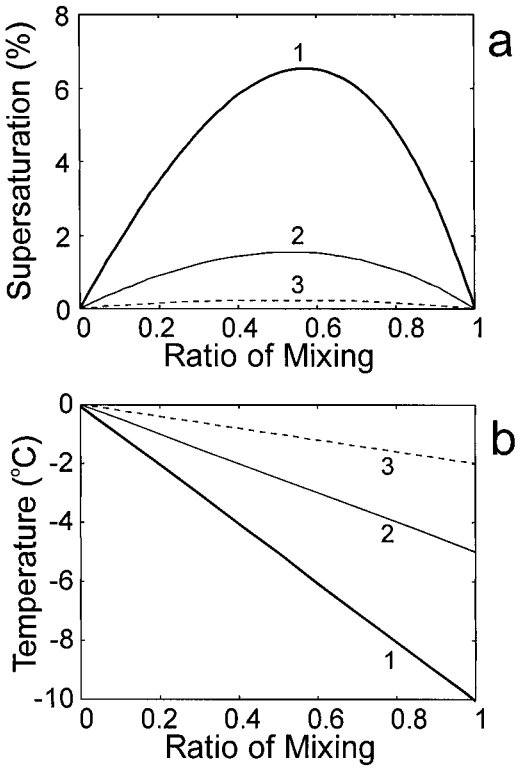

FIG. 1. Supersaturation (a) and temperature (b) vs the ratio of mixing, resulting from isobaric mixing of two saturated parcels having different temperatures. Initial temperatures of the volumes before mixing were 1) $T_1 = 0°C$, $T_2 = -10°C$; 2) $T_1 = 0°C$, $T_2 = -5°C$; 3) $T_1 = 0°C$, $T_2 = -2°C$.

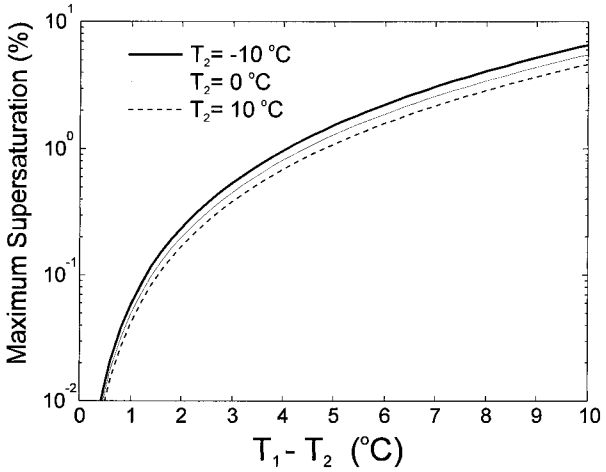

FIG. 2. The maximum supersaturation that can be reached from mixing two saturated volumes having different temperatures T_1 and T_2 vs the temperature difference $(T_1 - T_2)$.

be reached after mixing two saturated volumes versus the temperature difference $\Delta T = T_1 - T_2$ for different temperatures T_2. The supersaturation may reach more than 0.5% if the temperature difference between the two saturated volumes exceeds 3°C. As seen from Fig. 2, for the same ΔT, the maximum supersaturation increases with a decrease in temperature T_2.

The high supersaturation resulting from isobaric mixing requires two saturated volumes having different temperatures. How may this situation occur in a cloud? As described below, there are several possible scenarios of how two saturated volumes with different temperatures may form at the same cloud level.

3. Formation of high supersaturation in the vicinity of in-cloud temperature inversions

Vertical motions in a cloud having a lapse rate different from pseudoadiabatic may lead to the formation of saturated volumes with different temperatures at the same cloud level.

Consider a vertically moving turbulent parcel. The ''turbulent parcel'' implies an air continuum with a size much larger than the Kolmogorov viscosity microscale and consisting of a conglomerate of coherent parcels. This is what Hinze (1959, p. 276) called a ''fluid lump'' or what Telford et al. (1984) defined as a ''turbulent entity.'' Such a turbulent parcel may ascend or descend some distance before mixing with the cloud environment. The mixing is a cascading process of breakdown of turbulent eddies from the large scale down to the Kolmogorov microscale. After each breakdown, newly formed turbulent parcels still contain unmixed cores. All processes related to turbulent parcels in unmixed cores can be considered adiabatic to a good approximation. The characteristic time of mixing can be estimated as

$$\tau_t = (l^2/\varepsilon)^{1/3}, \tag{5}$$

where l is the characteristic size of the parcel and ε is the turbulent energy dissipation rate. In stratiform clouds, ε is typically 10^{-3}–10^{-4} m^2 s^{-3} (MacPherson and Isaac 1977; Mazin et al. 1984). From Eq. (5), a parcel of characteristic scale $l \sim 10^2$ m has a typical time of mixing τ_t on the order of 10^2–10^3 s. The following analysis considers processes with a typical time of $\tau < \tau_t$.

The temperature inside the cloud turbulent parcel will change along a pseudoadiabate before it mixes with the cloud environment. Hence, after ascending or descending for some distance, the temperature in the turbulent parcel and the cloud neighborhood will be different (Fig. 3). The temperature difference can be represented as

$$\Delta T(z) = T(z) - T(z_0) + \gamma_{\text{wet}}\Delta z, \tag{6}$$

where $\Delta z = z - z_0$ is the distance between two levels z and z_0; γ_{wet} is the pseudoadiabatic lapse rate; $T(z_0)$, $T(z)$ are the cloud temperature at levels z_0 and z, respectively.

The droplets inside the turbulent parcel will evaporate during descent and grow during ascent, maintaining the parcel close to water saturation. Thus, after a vertical displacement at some level z, such that $z \geq z_{\text{ev}}$, two

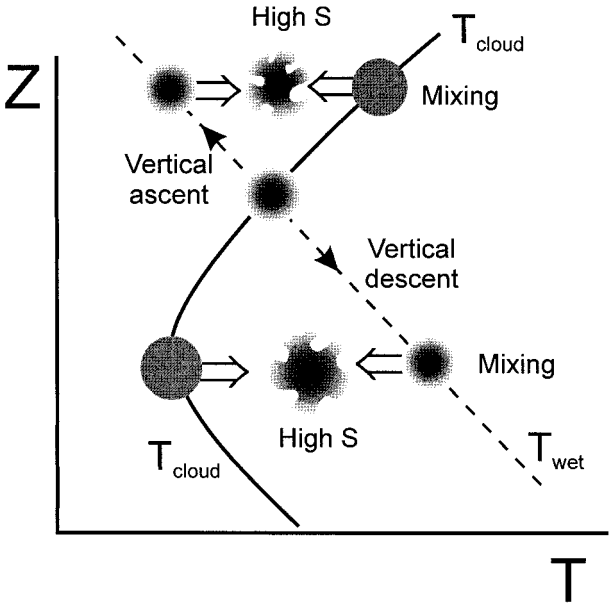

FIG. 3. Schematic for the formation of zones of high supersaturation in a cloud layer with a temperature inversion.

saturated volumes (i.e., the turbulent parcel and the cloud neighborhood) will have different temperatures. The value, z_{ev}, defines the level of total evaporation (Korolev and Mazin 1993):

$$\Delta z_{ev} = z_0 - z_{ev} = \frac{W(z_0)}{\beta_{ad}}. \tag{7}$$

Here, $W(z_0)$ is a liquid water mixing ratio (g kg^{-1}) at cloud level z_0, from which the turbulent parcel starts the vertical motion; β_{ad} is an adiabatic vertical gradient of liquid water mixing ratio

$$\beta_{ad} = \left(\frac{dW}{dz}\right)_{ad} = \frac{g\left[\dfrac{LR_m}{c_{pm}R_v T} - 1\right]}{\dfrac{(P - E_s)^2 R_v}{PR_a E_s}\left[1 + \dfrac{L^2 R_m E_s}{c_{pm}R_v^2 T^2 (P - E_s)}\right]}; \tag{8}$$

E_s is the saturation water vapor pressure at temperature T; L is the latent heat of condensation; c_{pm} is the specific heat of moist air; R_m, R_v, R_a, are the specific gas constants of moist air, water vapor, and dry air, respectively, and g is acceleration due to gravity. For $P = 900$ mb, $T = 273$ K, and $W = 0.1$ g kg^{-1}, Eqs. (7) and (8) yield $\beta_{ad} = 1.6 \times 10^{-3}$ g kg^{-1} m^{-1} and $\Delta z_{ev} \approx 60$ m.

If $z < z_{ev}$, then the total evaporation of all droplets occurs, and the temperature starts to change along a dry adiabat. In this case the above discussion is not applicable, since below the level z_{ev} the air inside the descending parcel is not saturated anymore. However, as it will be shown in section 4, the isobaric mixing of saturated and unsaturated volumes still may result in a high supersaturation.

The above mechanism is most effective in zones with in-cloud temperature inversions (see Fig. 3). Temperature inversions are frequently observed near cloud tops of stratus (St), altostratus (As), and nimbostratus (Ns) clouds and can range from 1° to 10°C or even more per 100 m. Temperature inversions related to frontal surfaces are often embedded in Ns. Observations of frontal clouds during the Canadian Freezing Drizzle Experiments (CFDE) I and III (Isaac et al. 1998) showed that the embedded temperature inversions might reach a depth of 1–2 km where the temperature was increasing by 15°C. Depending on the temperature profile, a vertical displacement of about 100 m may be enough to reach a temperature difference of several degrees centigrade. Turbulent fluctuations generated by wind shear may force cloud parcels to move up and down against the buoyancy forces within a thermally stable layer and particularly within layers with temperature inversions. This may explain why in some cases drizzle is associated with wind shear (e.g., Pobanz et al. 1994). However, Pobanz et al. also showed that drizzle was observed without an unstable wind shear in about 30% of the cases. Wind shear is not the only reason that may force cloud parcels to move up and down. Gravity waves, embedded convection, or cloud-top radiative instability can also generate vertical turbulent fluctuations.

4. Entrainment and isobaric mixing as a source of high supersaturation

The isobaric mixing of entrained dry and saturated cloudy air may result in high supersaturation zones. Consider the process of entrainment and mixing as a two-stage process. During the first stage, the entrained out-of-cloud dry parcel mixes with the cloud environment. Due to droplet evaporation, the air in the mixing volume reaches saturation. The next stage consists of the subsequent mixing of the saturated parcel with the cloud air. Depending on the temperature of the entrained parcel, the temperature of the saturated parcel after the first stage may be different from the cloud temperature. In this case, the subsequent mixing of this parcel with the cloud environment during the second stage will give a higher supersaturation. Figure 4 shows schematically the cascading process involving mixing of dry and cloudy air, giving rise to an increase in supersaturation.

The resulting supersaturation depends not only on the initial temperature difference, but also on the humidity of the entrained air and the cloud liquid water content (LWC). The equations for calculating the temperature and humidity in a mixed parcel are given in appendix B. Figure 5 shows the supersaturation, residual LWC, and temperature resulting from mixing cloudy air having different LWC and dry air with a humidity of 90%. The initial temperature difference before mixing was as-

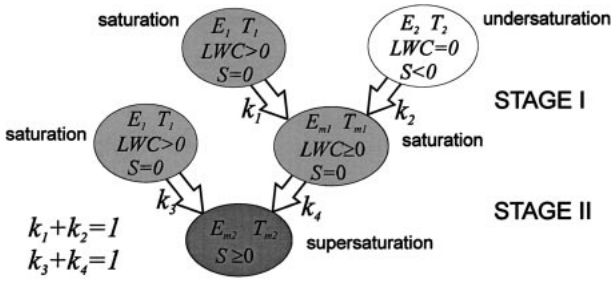

FIG. 4. Diagram explaining the two stages of isobaric mixing resulting in high supersaturation.

sumed as 5°C. After saturation is achieved, the following mixing with the cloud environment will result in a higher supersaturation and Eqs. (1)–(4) can be used to estimate supersaturation (see also Fig. 1). Depending on the ratio of mixing and LWC, the temperature in the mixed parcel after reaching saturation may be different from those in the cloud by up to 4°C (Fig. 5). Such a temperature difference is enough for isobaric mixing to generate zones with a supersaturation of about 1%.

Note that for larger LWC, a smaller ratio of mixing is needed to reach saturation in the mixed parcel, and thus a larger temperature difference between the cloud and the mixed saturated parcel will be reached. This effect is clearly seen in Fig. 5. The additional cooling caused by evaporation of the liquid water can be estimated as $\Delta T = kL\Delta W\Delta c_p$ [Eq. (B1), Appendix B]. For this situation, ΔT is of the order of 10^{-1} °C. As indicated in section 2 (Fig. 1), such a temperature difference cannot cause a large effect on the resulting supersaturation. The high supersaturation ($S > 0.5\%$) in a mixed parcel can be reached due to an initial temperature difference in the unmixed parcels, but not due to evaporation of liquid water. To attain high supersaturation, the temperature of the dry parcel can be both higher or lower than that of the cloud parcel.

The suggested approach for entrainment and mixing is quite different from the hypothesis of inhomogeneous mixing (e.g., Latham and Reed 1977; Baker and Latham 1979). The discussion around the problem of the effect of entrainment and mixing on enhanced droplet growth has continued for more than two decades (e.g., Beard and Ochs 1993). The basic idea of this hypothesis involves inhomogeneous mixing, that is, the entrained dry air evaporates completely some of the droplets, while the rest of the droplets in the parcel do not change significantly. The result of this process is a droplet size distribution having the same shape as before mixing, but with a reduced droplet number concentration. During an ascent these droplets are assumed to grow faster, as compared to droplets having higher concentrations in unmixed parcels, because of less competition for water vapor.

The difference and similarity between the hypothesis of inhomogeneous mixing and the approach described in this section is as follows. Both mechanisms can be split into two steps: ''mixing → ascent'' for inhomogeneous mixing, and ''mixing → mixing'' for the current approach (see Fig. 4). The first steps in both cases are the same: evaporation of droplets and attaining saturation. The second step consists in reaching supersaturation, which potentially may enhance the droplet growth. However, the way supersaturation is attained is different. In the hypothesis of inhomogeneous mixing, the supersaturation is caused by an ascent. In the current approach, the supersaturation is caused by isobaric mixing of two saturated volumes having different temperatures (Fig. 4, stage II).

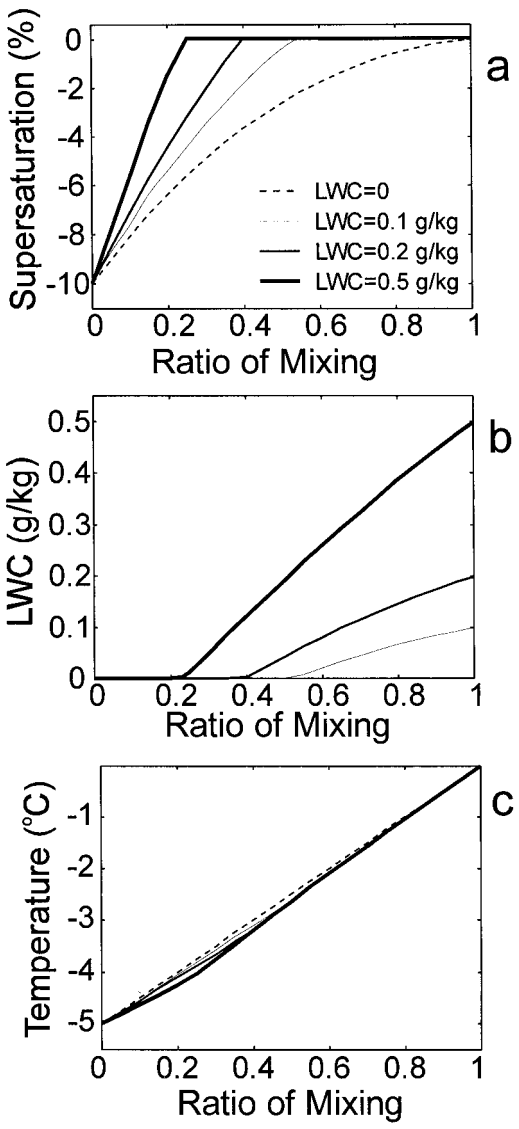

FIG. 5. (a) Supersaturation, (b) residual LWC, and (c) temperature formed during isobaric mixing of dry and cloud parcels (Fig. 3, stage 1). Calculations were made at $H = 1000$ m. The initial temperatures of the dry and cloud parcels were 0° and −5°C, respectively. The initial relative humidity of the dry volume was 90%.

5. Spatial structure of zones of high supersaturation

In sections 3 and 4 above, it was implied that the initial mass of the mixing parcel, M_p, is much smaller than that of the cloud layer, M_{cl}, where the mixing occurs, that is, $M_{cl} \gg M_p$. In this case, due to turbulent diffusion, the parcel will mix with a greater amount of cloudy air with time. Therefore, with time, the ratio of mixing will asymptotically approach $\lim_{t\to\infty} k = (M_{cl} - M_p)/(M_{cl} + M_p) \cong 1$. Such mixing would result in the vapor saturation being the same as in a cloud (Fig. 1). Hence, zones of high supersaturation caused by isobaric mixing can exist only in isolated zones and during a limited period of time before complete mixing within the cloud.

The spatial structure of zones of high supersaturation depends on the way the cloud parcels mix. Broadwell and Breidenthal (1982) summarized the experimental evidence and proposed the following description of mixing in turbulent shear layers. Mixing takes place in a series of events. Two shear layers of gas (liquid) exchange mass by engulfing parcels from an opposite layer into localized zones. The initially large-scale filaments of the two gases break down toward smaller scales due to the action of turbulence. The turbulence stretches the interface between the gases (liquids) and enhances the molecular diffusion across the increasing surface. The actual mixing of the engulfed volume is a molecular diffusion process that is most effective after the breakdown volumes reduce to the Kolmogorov viscosity scale. The time necessary to complete molecular diffusion defines the lifetime of the high supersaturation zones. This time can be estimated as a characteristic time of molecular diffusions,

$$\tau_d \sim \lambda_k^2/\nu, \tag{9}$$

where ν is the viscosity coefficient of air, $\lambda_k \sim (\nu^3/\varepsilon)^{1/4}$ is the Kolmogorov viscosity scale ($\lambda_k \sim 10^{-3}$ m for the troposphere), and ε is the turbulent energy dissipation rate. Assuming $\varepsilon = 10^{-3}$–10^{-4} m^2 s^{-3} Eq. (9) yields $\tau_d \sim 10^{-1}$ s. Since the ratio of mixing k changes from 0 to 1 across the interface, the maximum supersaturation is reached somewhere inside the interface where k is close to 0.5 (Fig. 1).

Based on this conceptual model of mixing, the high supersaturations are associated with zones of molecular mixing, and they have a characteristic size λ_k of the order of millimeters with a characteristic lifetime near tenths of a second. These finescale zones of high supersaturation are continuously appearing and vanishing during the event of mixing in different locations of a mixing parcel.

It is worth mentioning the principal difference between the spatial structure of supersaturation in a vertically moving adiabatic parcel, and in a parcel formed during isobaric mixing. In a vertically moving parcel, the supersaturation depends on the vertical velocity, u_z, and the time of phase relaxation, $\tau_p = A/n\bar{r}$ (Mazin 1966; Paluch and Knight 1984), where n is the droplet number concentration, $\bar{r}$ is the average droplet radius, A is a coefficient dependent on pressure and temperature. The time of phase relaxation defines the characteristic time of supersaturation changes due to condensation or evaporation of cloud droplets. The typical values of τ_p in liquid clouds are several seconds. As soon as the scalar fields of u_z and τ_p are uniform in a vertically moving parcel, the field of supersaturation at the timescale $t < \tau_t$ will be uniform as well. In the case of isobaric mixing, the field of supersaturation is highly nonuniform at the timescale $t < \tau_t$ in the zone of mixing. For the time $t > \tau_t$, when the mixing is complete, the field of supersaturation becomes uniform.

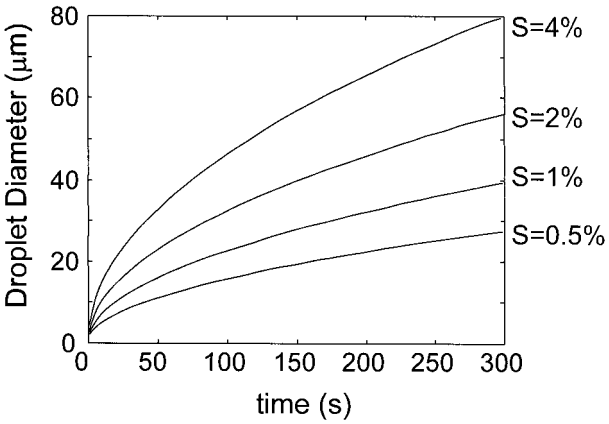

FIG. 6. Droplet growth by condensation at different supersaturations.

6. Droplet growth in zones of high supersaturation

Figure 6 shows the calculated droplet growth rate by condensation at different supersaturations. It is seen that with $S = 1\%$, droplets of 40 μm in diameter grow in 5 min. In the zones of isobaric mixing, this growth will not occur during one event. This time may be accumulated by some ''favored'' droplets during several pulses of supersaturation caused by mixing events. The probability of such an event is not high but may be enough to explain the concentrations of drizzle drops observed. After the favored droplets reach the 40-μm threshold, they can effectively continue further growth through collision–coalescence.

The spatial structure of supersaturation is of great importance for droplet population growth. Equations (1)–(4) show that the final result of isobaric mixing depends only on the initial temperatures in the mixing parcels and the ratio of mixing. In the absence of droplets, the resulting supersaturation at $t > \tau_t$ is independent of the type of mixing, that is, homogeneous or inhomogeneous. However, the presence of droplets makes the process of isobaric mixing more complex. The type

of mixing in this case may strongly affect the resulting droplet size distribution.

In the case of isobaric mixing, the high supersaturation exists in small zones at the interfaces between volumes with different temperatures. The peak supersaturation exists for a limited time at a particular point, since it moves with the interface attributed to a turbulent vortex. The residence time of droplets within these zones is limited by the lifetime of the zones. Because of the turbulent nature of mixing, the residence time and the supersaturation are different for different droplets. Therefore, the droplets are growing at different conditions and the time history of supersaturation $S(t, d_i)$ for each droplet d_i will be different. Among a variety of histories $S(t, d_i)$ there may exist a few favorable for rapid growth. During a relatively short time, these droplets may grow to drizzle size. The droplet size distribution in this case is expected to broaden with time. This process is closely linked to the theory of stochastic condensation (e.g., Kabanov et al. 1970; Stepanov 1976; Cooper 1989) explaining droplet spectrum broadening by fluctuations of supersaturation and the difference in the supersaturation history of different droplets. In these papers, the supersaturation fluctuations were governed by fluctuations of vertical velocity, and the spatial scale of these fluctuations was defined by the scale of vertical motions 10^1–10^2 m). However, in the suggested hypothesis, the nature of the supersaturation fluctuations is caused by isobaric mixing and its spatial scale is defined by the Kolmogorov viscosity microscale λ_k (10^{-3} m).

An important question arises in context of interstitial cloud condensation nuclei (CCN) activation and new droplet formation in the zones of high supersaturation. Newly activated droplets would slow down the growth of large droplets by condensation because of increased competition for water vapor. In this case the formation of precipitation embryo droplets may be significantly reduced. Droplet activation depends on the size and chemical composition of the interstitial CCN. The activation of CCN occurs if the supersaturation S_1 during the event of mixing exceeds the critical value S_{cr} (Mason 1957):

$$S_{cr} = 2\left(\frac{B}{3r_e}\right)^{3/2}. \tag{10}$$

Here, B is a correction coefficient on the equilibrium water vapor pressure over the droplet due to surface curvature; $r_e = r_c(i\rho_c\mu_w/\rho_w\mu_c)^{1/3}$ is the effective size of the interstitial CCN; r_c is the radius of the dry soluble part of the CCN; i is the Vant Hoff coefficient ($i \simeq 2$); ρ_c, μ_c are the density and molecular weight of the cloud nuclear soluble substance; and ρ_w, μ_w, are the density and molecular weight of water.

Due to mixing with the cloud environment, the supersaturation in the considered zone after some time will drop down to the average cloud value S_2. If the supersaturation $S_2 > S_{eq}(r, r_e)$, then these droplets will survive and continue to grow. Otherwise they will evaporate. Here,

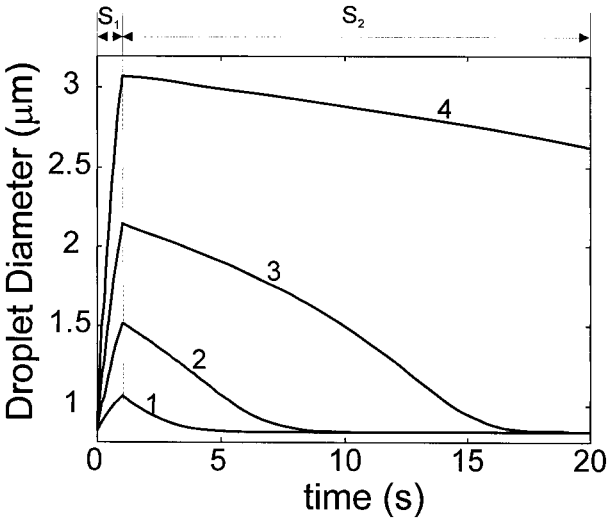

FIG. 7. Activation and evaporation of droplets during one cycle of increased (S_1) and decreased (S_2) supersaturation. 1) $S_1 = 0.2\%$; 2) $S_1 = 0.5\%$; 3) $S_1 = 1\%$; 4) $S_1 = 2\%$; $S_2 = 0.05\%$

$$S_{eq} = \frac{B}{r} - \frac{r_e^3}{r^3}. \tag{11}$$

If the lifetime of zones of high supersaturation is about 0.1 to 1 s, it may not be enough for the activation of droplets. Figure 7 shows the calculated changes of the size of a droplet exposed to a pulse of supersaturation. The supersaturation S_1 was maintained constant during 1 s (0.2%, 0.5%, 1%, and 2%) and then it was changed down to $S_2 = 0.05\%$ in a stepwise manner. The calculations were done for soluble CCN (NaCl) with a dry diameter of 0.1 μm. The initial droplet diameter was assumed to be equal to the equilibrium size $d_{eq} = 0.84$ μm at $S_2 = 0.05\%$. The example on Fig. 7 shows that 1 s at supersaturation $S_1 < 2\%$ is not long enough for the wetted CCN to exceed the equilibrium diameter and become a cloud droplet. Thus, short pulses of supersaturation may not activate interstitial CCN, although large droplets will keep growing under these conditions. This situation is favorable for enhanced large-droplet growth.

For the hypothesis of isobaric mixing, the activation of interstitial CCN is reduced due to the short duration of high supersaturation events. Such an approach gives an advantage as compared to the hypothesis of inhomogeneous mixing (Latham and Reed 1977; Baker and Latham 1979), which requires the ascent of the parcel after mixing event in order to promote the large droplet formation. The activation of interstitial CCN with radius r_e in an ascending parcel occurs, if the vertical velocity exceeds the critical value u_z^* (Korolev 1994):

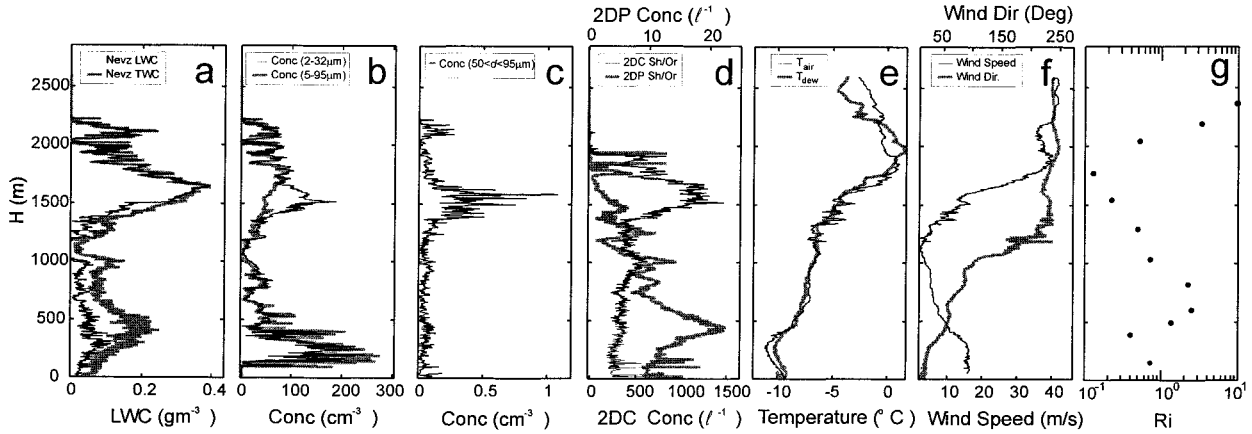

FIG. 8. Changes of microphysical and thermodynamical parameters with altitude measured in a drizzling supercooled nimbostratus associated with a frontal system during the Canadian Freezing Drizzle Experiment I on 9 March 1995, 1904:14–1921:40 UTC, Newfoundland. (a) liquid and total water content measured by the Nevzorov probe; (b) concentration of droplets in size ranges 3–47 μm and 5–95 μm measured by FSSPs; (c) concentration of large droplets (50–95 μm) measured by an FSSP; (d) evaluated concentration of drops measured by a PMS OAP-2DC (25–800 μg) and an OAP-2DP (200–6400 μm); (e) air and dewpoint temperatures; (f) wind speed and wind direction; (g) calculated Richardson number.

$$u_z^* = \frac{Gn\bar{r}}{\beta_{\text{ad}}(r_e)^{3/2}}. \tag{12}$$

Here, G is a coefficient dependent on pressure and temperature ($G = 1.2 \times 10^{-20}$ m$^{7/2}$ s^{-1} at $T = 0$°C). The value of u_z^* depends on interstitial CCN, droplet sizes, and number concentration. For typical values of $n\bar{r}$ and interstitial CCN (Hudson 1984), the characteristic values of u_z^* varies in clouds from 10^{-1} to 10^0 m s^{-1} (Korolev and Mazin 1993). Such values of regular and turbulent vertical velocities are typical in convective and stratiform clouds (MacPherson and Isaac 1977; Mazin et al. 1984). Therefore, the enhanced droplet growth of droplets for the hypothesis of inhomogeneous mixing would be most effective only when $u < u_z^*$. This may significantly limit the role of the inhomogeneous mixing mechanism in precipitation formation.

7. Experimental results

High supersaturation resulting from isobaric mixing is a frequent phenomenon, easily observed during our daily life. A fog on the top of a cup with hot coffee, or fog coming out as we exhale in cold weather are a result of CCN activation in zones of high supersaturation resulting from isobaric mixing. Below, we consider some experimental results from in situ measurements supporting the hypothesis of isobaric mixing.

a. Microphysical measurements near in-cloud inversions

Figure 8 presents some results of measurements of cloud microstructure during the (CFDE I; Isaac et al. 1998). The measurements were obtained using the National Research Council (NRC) Convair-580 well equipped for cloud microphysical measurements. Figure 8 shows the following: LWC measured by the LWC–TWC Nevzorov probe (Korolev et al. 1998); droplet number concentration from size ranges 2 to 32 μm and 5 to 95 μm in diameter measured by two different Particle Measuring System (PMS) Forward Scattering Spectrometer Probes (FSSP) (Knollenberg 1981); droplet concentration from size range 50–95 μm derived from the FSSP data; estimation of large particle concentration derived from a PMS OAP-2DC (25–800 μm) and OAP-2DP (200–6400 μm); air and dew point temperatures; wind speed and wind direction; and Richardson number. The measurements were obtained during a vertical sounding in a drizzling nimbostratus cloud associated with a frontal system.

The data show the growth of drizzle occurring near a temperature inversion associated with a wind shear layer. Thus, the maximum concentration of large droplets (50–95 μm) measured by the FSSP was observed at an altitude near 1600 m (Fig. 8c). This maximum agrees well with the location of the maximum concentration measured by the OAP-2DC (Fig. 8d), and it supports the FSSP data. Measurements by the OAP-2DP shows that the concentration of precipitating drops >200 μm increases toward the ground (Fig. 8d). This observation supports the hypothesis that once droplets reach the threshold diameter of 40–50 μm, their further growth in downward direction occurs through a collision–coalescence mechanism (e.g., Beard and Ochs 1993). The maximum concentration of large droplets (50–95 μm) is observed in the region of the temperature inversion (Fig. 8e) and the strong wind shear (Fig. 8f). The Richardson number at this altitude decreases down to 0.1 (Fig. 8g), which indicates the dynamical instability of this layer. This would be a favorable place for

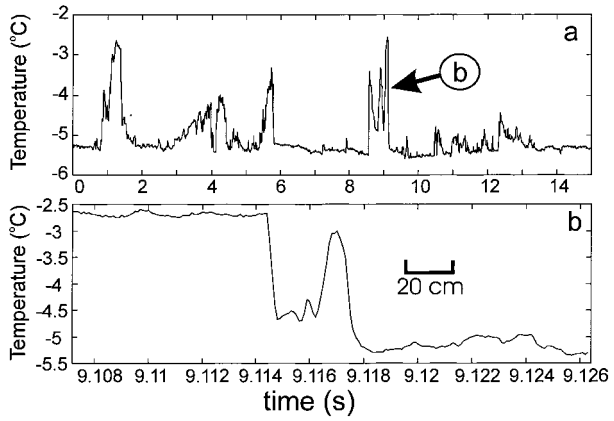

FIG. 9. Measurements of temperature fluctuations by the Ultrafast Airborne Thermometer in St of 09.02.1998 in Ottawa. (a) averaging interval 0.01 s; (b) temperature jump indicated by the arrow in Fig. 6a at time resolution 10^{-4} s.

isobaric mixing to occur. Many other such examples can be found using the data from CFDE I and III.

b. In-cloud temperature measurements in the vicinity of temperature inversions

Figure 9 shows the measurements of small-scale fluctuations of temperature in St cloud capped by a temperature inversion of about 10°C. The measurements were made using the Ultrafast Airborne Thermometer (Haman et al. 1997a,b) installed on the NRC Convair-580 during CFDE III. The Ultrafast Airborne Thermometer was modified for use in icing conditions at airspeeds up to 360–400 km h^{-1}. Figure 9a shows the temperature fluctuations with an amplitude near 2.5° to 3°C. Such temperature differences are enough for isobaric mixing to generate zones with a supersaturation of 0.5% to 0.7%. Figure 9b shows the zoomed transition through the temperature jump at time resolution 10^{-4} s indicated on Fig. 9a by the arrow. It is seen that the temperature drops 2°C inside cloud along a distance of about 4 cm. Haman et al. (1997a,b) have observed such temperature jumps in many convective nonsupercooled clouds in the past. The existence of these temperature interfaces provides support for the hypothesis of isobaric mixing.

8. Conclusions

The mechanism of enhanced growth of large droplets due to isobaric mixing can be applied to both stratiform and convective clouds. In stratiform clouds, an effective source of cloud volumes having temperatures different from the cloud environment can be in-cloud or cloud-top inversions. In convective clouds, the volumes with different temperatures may be generated by entrainment.

Gerber (1991) discussed transient supersaturations observed in fogs and used the nongradient mixing concept of saturated parcels having different temperature to grow the large drops that were observed. In this work Gerber assumed the ratio of mixing k = const during a mixing event and the mixing was considered at $t > \tau_t$, that is, when molecular mixing is completed. Such conditions look artificial since the value of k during mixing continuously changes and with time k approaches 1, as was discussed in section 5. This consideration is only applicable for mixing inside a volume with isolated boundaries rather than for a cloud with infinite borders.

The hypothesis of isobaric mixing may explain the rapid growth of large droplets and the formation of drizzle in warm clouds. In the special case of freezing drizzle, slow-droplet growth increases the probability of droplet freezing and prevents large-droplet formation. However, freezing drizzle often occurs via the condensation–coalescence mechanism (Cober et al. 1996; Isaac et al. 1998). This hypothesis may also help explain the observations of both drizzle cells (Vali et al. 1998) and large-droplet formation near cloud tops in shallow stratiform decks. The necessary conditions for drizzle formation using the hypothesis of isobaric mixing are (i) the presence of a temperature inversion and (ii) a mechanism that triggers mass exchange and mixing between two layers with different temperatures (e.g., a dynamically unstable wind shear layer, Kelvin–Helmholtz or gravity waves, or embedded convection). Figure 10 shows a schematic diagram of drizzle formation in a stratiform cloud in the presence of a temperature inversion.

In future studies, consideration should be given to determining the characteristic time of droplet growth to 40-μm threshold diameter in the mixing zones. Approximately $\tau_{gr} = 200$ s is required for a droplet to grow from 20 to 40 μm under a supersaturation $S = 1\%$ (Fig. 6). If we assume the duration of the high supersaturation event is $\tau_d = 0.1$ s, then the number of events required for the droplet growth would be $N = \tau_{gr}/\tau_d = 2000$. If the droplet experiences one high supersaturation event during a mixing event, then the droplet would accumulate the time necessary for the growth during $t = N\tau_t$. Assuming $\tau_t = 10^2$ s [Eq. (5)] we get $t \sim 60$ h. On the other hand, if the droplet is continuously moving from one supersaturation event into another and, thus, always staying in a zone of high supersaturation, then $t = \tau_{gr} = 200$ s. The above two estimations give the growth time between 3 min and greater than 60 h. The actual growth time is somewhere in between these two extremes. The key question in this consideration is how many times the droplet may experience high supersaturation events during one mixing event. This question can be answered using laboratory or numerical modeling.

The simulation of droplet growth in molecular mixing zones with volumes of different temperatures can be performed using linear-eddy models (e.g., Krueger 1993). Such studies are currently being conducted with some success (P. Austin 1998, personal communication).

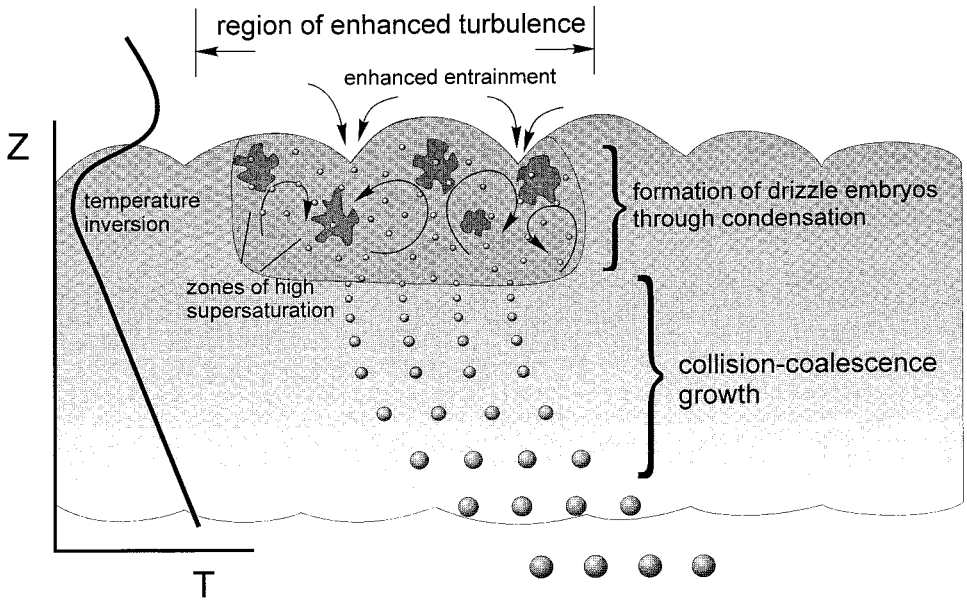

FIG. 10. Schematic diagram of enhanced droplet growth due to isobaric mixing in the presence of a temperature inversion.

The suggested hypothesis does not reject the role of giant nuclei, recirculation, and inhomogeneous mixing in drizzle formation in stratiform clouds, but rather supplements and revises their role. The contribution of each of these effects may be different in different clouds and dependent on the type of air mass, CCN distribution, and thermodynamic parameters inside and outside of the cloud layer.

Acknowledgments. The authors acknowledge Prof. Krzysztof Haman of the Warsaw University, Poland, for participation in the Canadian Freezing Drizzle Experiment and for providing measurements by the Ultrafast Airborne Thermometer. Funding for this work was provided by the National Search and Rescue Secretariat. The authors are grateful for the efforts of the National Research Council during the Canadian Freezing Drizzle Experiment.

APPENDIX A

Supersaturation Resulting from Isobaric Mixing of Two Saturated Parcels

Consider two air volumes with vapor mixing ratios q_1 and q_2 (mass of water vapor per unit mass of dry air). Assume a k_1 portion of the first volume mixes with a k_2 portion of the second volume, such that $k_1 + k_2 = 1$. The vapor mixing ratio q_m in the mixed volume will be

$$q_m = k_1 q_1 + k_2 q_2. \tag{A1}$$

The vapor pressure E_m in the mixed volume can be derived from Eq. (A1) by substituting k_2 and $q = [E/(P - E)](R_a/R_v)$ as

$$E_m = P\frac{k_1 + \dfrac{E_2(P - E_1)}{P(E_1 - E_2)}}{k_1 + \dfrac{(P - E_1)}{(E_1 - E_2)}}; \tag{A2}$$

here E_1, E_2 are the water vapor pressures in the first and second before mixing volumes, respectively; P is the moist air pressure (P = const during mixing); and R_v, R_a, are the specific gas constants of water vapor and dry air, respectively.

The temperature of the mixed volume can be found from the law of energy conservation:

$$k_1(q_1 c_{pv} + c_{pa})(T_1 - T_m) = k_2(q_2 c_{pv} + c_{pa})(T_m - T_2); \tag{A3}$$

here T_1, T_2 are the temperatures in first, second volumes, respectively; and c_{pv}, c_{pa} are the specific heat capacitance of water vapor and dry air at constant pressure, respectively.

Similarly as in Eqs. (A1) and (A2), substituting q_1, q_2, and k_2 we obtain

$$T_m = \frac{k_1 T_1 + a(1 - k_1)T_2}{k_1 + a(1 - k_1)}, \tag{A4}$$

here

$$a = \frac{1 + \dfrac{c_{pv}R_aE_2}{c_{pa}R_v(P - E_2)}}{1 + \dfrac{c_{pv}R_aE_1}{c_{pa}R_v(P - E_1)}}. \quad \text{(A5)}$$

The resulting supersaturation after mixing the two volumes will be

$$S_m = \frac{E_m}{E_S(T_m)} - 1, \quad \text{(A6)}$$

where $E_s(T_m)$ is the saturated vapor pressure at temperature T_m.

APPENDIX B

Supersaturation Resulting from Isobaric Mixing of Dry and Saturated Parcel with Nonzero LWC

Consider the mixing of dry and saturated cloudy parcels with nonzero LWC as a two-step process. First, dry air mixes with a cloudy air. Second, if the resulting humidity is below saturation, then liquid water evaporates until either saturation of the parcel or total evaporation of the liquid water occurs. The vapor pressure and temperature resulting from the first step can be found from Eqs. (A1)–(A6). To find the result of the second step, the following system of three equations should be solved:

$$T_m = T_{m0} - \frac{\Delta WL}{c_{pa} + (q_{m0} + \Delta W)c_{pv}}, \quad \text{(B1)}$$

$$E_m = \frac{(q_{m0} + \Delta W)PR_v}{R_a + (q_{m0} + \Delta W)R_v}, \quad \text{(B2)}$$

$$E_m \le E_{S0} \exp\left[\frac{L}{R_v}\left(\frac{1}{T_0} - \frac{1}{T_m}\right)\right]. \quad \text{(B3)}$$

Here T_{m0}, q_{m0} are the temperature and vapor mixing ratio after mixing of two volumes, but before evaporation of liquid water; E_{s0} is the saturated water vapor pressure at temperature T_0; W is the liquid water mixing ratio; and ΔW is evaporated liquid water mixing ratio. The values T_{m0}, q_{m0} can be found from Eqs. (A1)–(A5). It follows that $\Delta W \le kW$, that is, the evaporated water cannot exceed that available in the cloud parcel, here $k = k_1$ (or k_2). The first and second equations describe changes in temperature and vapor pressure due to evaporation of the liquid water ΔW. The third equation shows the condition that the resulting humidity cannot exceed the saturated one. The system of Eqs. (B1)–(B3) was solved numerically.

REFERENCES

Baker, M. B., and J. Latham, 1979: The evolution of droplet spectra and rate of production of embryonic raindrops in small cumulus clouds. *J. Atmos. Sci.*, **36,** 1612–1615.

Beard, K. V., and H. T. Ochs III, 1993: Warm rain initiation: An overview of microphysical mechanisms. *J. Appl. Meteor.*, **32,** 608–625.

Bohren, C. F., and C. H. Albrecht, 1998: *Atmospheric Thermodynamics*. Oxford University Press, 402 pp.

Broadwell, J. E., and R. E. Breidenthal, 1982: A simple model of mixing and chemical reaction in a turbulent shear layer. *J. Fluid Mech.*, **125,** 397–410.

Cober, S. G., J. W. Strapp, and G. A. Isaac, 1996: An example of supercooled drizzle droplets formed through a collision coalescence process. *J. Appl. Meteor.*, **35,** 2250–2260.

Cooper, W. A., 1989: Effect of variable droplet growth histories on droplet size distributions. Part I: Theory. *J. Atmos. Sci.*, **46,** 1301–1311.

Gerber, H., 1991: Supersaturation and droplet spectral evolution in fog. *J. Atmos. Sci.*, **48,** 2569–2588.

Haman, K. E., A. Makulski, and S. P. Malinovski, 1997a: A new ultrafast thermometer for airborne measurements in clouds. *J. Atmos. Oceanic Technol.*, **14,** 217–227.

——, S. P. Malinowski, and R. Busen, 1997b: Ultrafast aircraft thermometer. *Proc. WMO Workshop on Measurements of Cloud Properties for Forecasts of Weather Climate*, Rep. 30, Mexico City, Mexico, WMO, 116–124.

Hinze, J. O., 1959: *Turbulence. An Introduction to its Mechanism and Theory*. McGraw-Hill, 586 pp.

Hudson, J. G., 1984: Cloud condensation nuclei measurements within clouds. *J. Climate Appl. Meteor.*, **23,** 42–51.

Isaac, G. A., S. G. Cober, A. V. Korolev, J. W. Strapp, A. Tremblay, and D. L. Marcotte, 1998: Overview of the Canadian Freezing Drizzle Experiment I, II, and III. Preprints, *Conf. on Cloud Physics*, Everett, WA, Amer. Meteor. Soc., 447–450.

Kabanov, A. S., I. P. Mazin, and V. I. Smirnov, 1970: The effect of the spatial inhomogeneity newly-formed drops on their size spectrum in a cloud. *Izv. Acad. Sci. USSR, Atmos. Oceanic Phys.*, **6,** 149–155.

Knollenberg, R. G., 1981: Techniques for probing cloud microstructure. *Clouds, Their Formation, Optical Properties, and Effects*, P. V Hobbs and A. Deepak, Eds., Academic Press, 15–92.

Korolev, A. V., 1994: A study of bimodal droplet size distribution in stratiform clouds. *Atmos. Res.*, **32,** 143–170.

——, and I. P. Mazin, 1993: Zones of increased and decreased droplet number concentration in stratiform clouds. *J. Appl. Meteor.*, **32,** 760–773.

——, J. W. Strapp, G. A. Isaac, and A. N. Nevzorov, 1998: The Nevzorov airborne hot-wire LWC–TWC probe: Principal of operation and performance characteristics. *J. Atmos. Oceanic Technol.*, **15,** 1495–1510.

Krueger, S. K., 1993: Linear eddy modeling and mixing in stratus clouds. *J. Atmos. Sci.*, **50,** 3078–3090.

Latham, J., and R. L. Reed, 1977: Laboratory studies of the effect of mixing on the evolution of cloud droplet spectra. *Quart. J. Roy. Meteor. Soc.*, **103,** 279–306.

MacPherson, J. I., and G. A. Isaac, 1977: Turbulent characteristics of some Canadian cumulus clouds. *J. Appl. Meteor.*, **16,** 81–90.

Mason, B. J., 1957: *The Physics of Clouds*. Oxford, 481 pp.

Mazin, I. P., 1966: The stochastic condensation and its effect on the formation of cloud drop size distribution. *Proc. Int. Conf. on Cloud Physics*, Toronto, ON, Canada, IAMAP, 67–71.

——, V. I. Silaeva, and M. A. Strunin, 1984: Turbulent fluctuations of horizontal and vertical wind velocity components in various cloud forms. *Izv. Acad. Sci. USSR, Atmos. Oceanic Phys.*, **20,** 6–11.

Paluch, I. R., and C. A. Knight, 1984: Mixing and the evolution of cloud droplet size spectra in a vigorous continental cumulus. *J. Atmos. Sci.*, **41,** 1801–1805.

Pobanz, B. M., J. D. Marwitz, and M. K. Politovitch, 1994: Conditions associated with large drop region. *J. Appl. Meteor.*, **33,** 1366–1372.

Rogers, R. R., 1976: *A Short Course in Cloud Physics.* Pergamon Press, 227 pp.

Stepanov, A. S., 1976: Influence of turbulence on the size spectrum of cloud drops during condensation. *Izv. Acad. Sci. USSR, Atmos. Oceanic Phys.,* **12,** 167–173.

Telford, J. W., T. S. Keck, and S. K. Chai, 1984: Entrainment at cloud tops and the droplet spectra. *J. Atmos. Sci.,* **41,** 3170–3179.

Vali, G., R. D. Kelly, J. French, S. Haimov, D. Leon, R. E. McIntosh, and A. Pazmany, 1998: Finescale structure and microphysics of coastal stratus. *J. Atmos. Sci.,* **55,** 3540–3564.